

MHD Pulsatile Flow Through a Porous Channel with Heat Generation

Promise Mebine^{1*} and Liberty Ebiwareme²

¹Department of Mathematics and Computer Science, Niger Delta University, Wilberforce Island, Bayelsa State, Nigeria.

²Department of Mathematics, Rivers State University of Science and Technology, Nkpolu-Oroworukwo, Port Harcourt, Rivers State, Nigeria.

Author's contribution

This work was carried out in collaboration between both authors. Author PM designed the study, performed the mathematical formulations, computed the graphical illustrations, did the analyses and wrote the first draft of the manuscript and managed literature searches. Author LE proffered the solutions of the study and managed literature searches. Both authors read and approved the final manuscript.

Article Information

DOI: 10.9734/ARJOM/2017/32734

Editor(s):

(1) Hamidah Ibrahim, Department of Computer Science, Universiti Putra Malaysia, Malaysia.

Reviewers:

(1) Sami Ullah Khan, International Islamic University, Pakistan.

(2) P. A. Murad, Vienna, VA, USA.

Complete Peer review History: <http://www.sciencedomain.org/review-history/18651>

Received: 13th March 2017

Accepted: 3rd April 2017

Published: 15th April 2017

Original Research Article

Abstract

The paper considers the investigation of MHD oscillatory flow initiated by pulsatile pressure gradient in the presence of heat generation in a channel with perforated walls. Analytical solutions of the flow variables are derived from the governing set of dimensionless momentum and energy equations together with the accompanying boundary conditions via quasi-steady-state solution assumption. The results are discussed quantitatively with graphical illustrations with various physical parameters such as Magnetic, M ; Heat generation, H ; Free convection, Gr ; phase angle or pulsation factor, $\Omega \tau$ and the wall temperature ratio, m for respective Prandtl numbers, $Pr = 0.71$ (air), $Pr = 7$ (water) and $Pr = 21$ (human blood). The results showed sensitive dependence on the parameters such that increasing Magnetic parameter, decreases maximum velocity in the channel with flow reversals seen near the centre of the channel; increasing Heat source, introduces

*Corresponding author: E-mails: p.mebine@yahoo.com, pw.mebine@ndu.edu.ng;

non-smooth flow in the maximum velocity with temperature oscillations in the fluid of the channel; increasing thermal buoyancy force, increases the velocity in the channel with reversal for a given phase angle; the maximum velocity in the channel increases with increasing wall temperature ratio, and both Suction, and Injection, introduced upturn and downturn of the velocity and temperature, thereby physically signifying the oscillatory effect of the pressure gradient.

Keywords: Analytical; heat generation; human blood; MHD; pulsatile flow; porous.

2010 Mathematics Subject Classification: 37C55, 76Z05, 82D40, 92C35, 35Q35.

1 Introduction

The study of the flow between parallel plates generated by a pulsatile pressure gradient has dated back to several decades due to many applications found in bio-mechanics, bio-physics, physiology and medical engineering. A pulsatile flow is well known in fluid dynamics, and it is simply defined as a fluid flow with periodic variations or oscillations, or known as Womersley flow. Berman [1] and Wang [2] investigated the velocity distribution and shear stresses in an infinite channel. A major application of such studies is to the understanding of the dialysis of blood in artificial kidneys [3]. The MHD flow between parallel two porous plates has various applications in MHD power generators, MHD pumps, aerodynamic heating. The studies of MHD flows have taking a centre-point in research due to its applications in hemodynamics and the likes of MRI technology [4].

It is known that the study of the fluids that reveal oscillatory flows have numerous important applications in science and nature. There are quite a number of abounding well known and common examples in medical sciences such as blood flow through an artery, peristaltic food motion in the intestine and motion of urine in the urethra. In astrophysical and geophysical studies, theoretical and experimental explorations have taken a look at the direction of stellar shapes, cores of terrestrials and sun plasma for the inducing factors of oscillatory motions. Vardanyan [5] had developed several theoretical models on the influence of magnetic strength of pulsatile type flow. It has been asserted that the presence of consistent and uniform magnetic strength leads to decrease the flow rate, and it was stated that the work has a significant impact on biological research. More still, there are lots of fascinating studies relating to oscillatory flows, which have been considered by researchers in recent times. Ali et al.[6] examined the study of hydromagnetic flow and heat transfer of a Jeffrey fluid in an oscillatory surface; Khan et al.[7] considered hydromagnetic flow and heat transfer over a porous oscillating stretching surface in a viscoelastic fluid with porous medium; Ali et al. [8] presented the problem of unsteady flow of third grade fluid over an oscillatory stretching sheet with thermal radiation and heat source/sink; Khan et al.[9] presented the case of Soret and Dufour effects on hydromagnetic flow of viscoelastic fluid over porous oscillatory stretching sheet with thermal radiation; Khan et al. [10] also studied the problem of influence of heat generation/absorption with convective heat and mass conditions in unsteady flow of Eyring Powell Nanofluid over porous oscillatory stretching surface. Further, Ali et al. [11] studied MHD flow and heat transfer of couple stress fluid over an oscillatory stretching sheet with heat source/sink in porous medium; Khan et al. [12] presented the study of Soret and Dufour effects on hydromagnetic flow of Eyring Powell fluid over an oscillatory stretching surface with heat generation/absorption and chemical reaction. The most recent studies are slip effects in the hydromagnetic flow of a viscoelastic fluid through porous medium over a porous oscillatory stretching sheet [13]; unsteady hydromagnetic flow of Oldroyd-B fluid over an oscillatory stretching surface [14]. There are diverse methods of solution for these studies, ranging from analytical to numerical. Ali et al. [15] utilized Legendre wavelets method to tackle the problem of a third grade fluid flow and forced convection in a porous duct of parallel plates.

On the other hand, heat generation has applications in industrial pollutions, bio-systems and many more. Modelling of hyperthermia-induced temperature distribution requires an accurate description of the mechanism of heat transfer. It is reported in Dewhirst and Samulski [16] that blood flow affects the thermal response of living tissues. The heat exchange between living tissues and blood network that passes through it depends on the geometry of the blood vessels and the flow variation of blood. Craciunescu and Clegg [17] studied the effect of oscillatory flow upon the resulting temperature distribution of blood and convective heat transfer in rigid vessels. The importance of different types of blood vessels in the process of bio-heat transfer has been intensively studied [18, 19].

Recently, MHD pulsatile flow of engine oil based carbon nanotubes between two concentric cylinders with oscillating pressure gradient was investigated by Haq et al. [20]. It was demonstrated in their studies that the flow of blood and pressure can be managed sufficiently by the application of an external magnetic field to serve as a guide to abate some arterial diseases. To this end, there is no gainsaying that flows within channels and vessels for the studies of bio-heat transfer, bio-mechanics, bio-physics, physiology and medical engineering are controlled in order to achieve effective and reliable output for the specific applications. MHD is generally known to play a vital role in that direction. In practical terms, it is known that channel walls are of different temperatures. Mebine [21] stated that this is of primary importance in the study of hydromagnetic flows with heat transfer in channels or between parallel plates such that temperature ratio is being generated between the wall temperatures and that of the ambient temperature. No mention has been made of temperature ratio effect of all the studies considered above in this work. Therefore, it is the objective of this work to consider the effect of MHD on the oscillatory flow initiated by pulsatile pressure gradient in the presence of heat generation in a channel with perforated walls effected by temperature ratio. The sections that follow hereafter are the Mathematical Formulations, Method of Solution, Discussion of Results, and Concluding Remarks.

2 Mathematical Formulations

The physical problem consists of a MHD flow through a horizontal channel with perforated walls. The flow is driven by a prescribed oscillatory axial pulsatile pressure applied across the ends of the channel and is given by Burton [22] and Bestman [23]

$$-\frac{\partial p}{\partial x} = \alpha_0 + \alpha \cos \omega t, \quad (2.1)$$

where α_0 and α are the steady component of the pressure gradient and pulsatile component, respectively. In this work, the steady component is assumed zero. The plate at $y = 0$ is maintained at temperature T_0 while fluid is blown to it with velocity V_0 , and at $y = h$ is kept at temperature T_h and fluid is sucked from it with the velocity V_0 . It is stated here that all the fluid properties are assumed constant, except for the density in the buoyancy force term, which varies according to the law

$$\rho = \rho_\infty - \rho_\infty \beta (T - T_\infty). \quad (2.2)$$

This is Boussinesq approximation in which β represents the coefficient of volume expansion. Subscript ∞ refers to conditions in the undisturbed fluid.

Under this condition the following equations are obtained:

$$v = -V_0, \quad (2.3)$$

$$\frac{\partial u}{\partial t} + v \frac{\partial u}{\partial y} = -\frac{1}{\rho_\infty} \frac{\partial p}{\partial x} + \nu \frac{\partial^2 u}{\partial y^2} - \frac{\sigma_c B_0^2}{\rho_\infty} u + g\beta(T - T_\infty), \quad (2.4)$$

$$\frac{\partial T}{\partial t} + v \frac{\partial T}{\partial y} = \frac{\kappa}{\rho_\infty c_p} \frac{\partial^2 T}{\partial y^2} + \frac{Q}{\rho_\infty c_p} (T - T_\infty), \quad (2.5)$$

where u , velocity along the axial or x - axis; v , velocity along the normal or y -axis; t , time; p , pressure; ρ , fluid density; ν , kinematic viscosity; Q , total heat generation constant; σ_c , electrical conductivity of the fluid; B_0 , applied magnetic field strength; c_p , heat capacity at constant pressure; κ , thermal conductivity; T , fluid temperature, and g , acceleration due to gravity. The equations (2.4, 2.5) are subject to the boundary conditions

$$u = 0, T = T_0 \text{ at } y = 0, \quad (2.6)$$

$$u = 0, T = T_h \text{ at } y = h. \quad (2.7)$$

To facilitate the analyses of the problem, the following non-dimensional quantities are introduced:

$$\begin{aligned} X &= \frac{x}{h}, Y = \frac{y}{h}, U = \frac{hu}{\nu}, \tau = \frac{t\nu}{h^2}, \Omega = \frac{\omega h^2}{\nu}, \\ \theta &= \frac{T - T_\infty}{T_0 - T_\infty}, m = \frac{T_h - T_\infty}{T_0 - T_\infty}, P = \frac{h^2 p}{\rho_\infty \nu^2}, \\ S &= \frac{V_0 h}{\nu}, M = \frac{\sigma_c h^2 B_0^2}{\rho_\infty \nu}, Gr = \frac{g\beta h^3 (T_0 - T_\infty)}{\nu^2}, \\ H &= \frac{Qh^2 (T_0 - T_\infty)}{\rho_\infty c_p \nu}, Pr = \frac{\nu}{\alpha_d}, \alpha_d = \frac{\kappa}{\rho_\infty c_p}. \end{aligned} \quad (2.8)$$

Applying the equations (2.8), equations (2.4, 2.5) and (2.6, 2.7) are respectively transformed to

$$\frac{\partial U}{\partial \tau} - S \frac{\partial U}{\partial Y} = -\frac{\partial P}{\partial X} + \frac{\partial^2 U}{\partial Y^2} - MU + Gr\theta, \quad (2.9)$$

$$\frac{\partial \theta}{\partial \tau} - S \frac{\partial \theta}{\partial Y} = \frac{1}{Pr} \frac{\partial^2 \theta}{\partial Y^2} + H\theta, \quad (2.10)$$

subject to

$$U = 0, \theta = 1 \text{ at } Y = 0, \quad (2.11)$$

$$U = 0, \theta = m \text{ at } Y = 1. \quad (2.12)$$

Here the parameters entering the problem are m , wall temperature ratio; S , Suction parameter: $S > 0$, Suction and $S < 0$, Injection; M , Magnetic parameter; Gr , Grashof number; H , Heat Source: $H > 0$, Heat generation and $H < 0$, Heat loss; Pr , Prandtl number.

3 Method of Solution

The pressure gradient (2.1) depicts that it is oscillatory. Therefore, in order to obtain purely oscillatory flow, let the pressure gradient (2.1), the velocity and energy equations (2.9, 2.10) subject to the boundary conditions (2.11, 2.12) be written respectively as follows:

$$-\frac{\partial P}{\partial X} = \text{Re } \alpha \exp(I \Omega \tau), \quad (3.1)$$

$$U(Y, \tau) = \text{Re } \Phi(Y) \exp(I \Omega \tau), \quad (3.2)$$

$$\theta(Y, \tau) = \text{Re } \Theta(Y) \exp(I \Omega \tau), \quad (3.3)$$

where $I = \sqrt{-1}$ and Re means the real part of a complex variable. The equations (3.1) - (3.3) are quasi-steady-state solutions [24], which are used mostly to visualize the basic concept of boundary layer in unsteady flows, where exact solutions of the Navier-Stokes equations are sorted for when objects are subjected to cosinusoidal oscillations for specific physical applications. Therefore, the solutions of the velocity and energy equations (2.9, 2.10), by reason of equations (3.1) - (3.3) are respectively obtained as follows:

$$\begin{aligned}
 U = & \frac{\alpha}{M + I\Omega} \exp(I\Omega\tau) - \frac{Gr(m - \exp(r2))}{(\exp(r1) - \exp(r2))[r1^2 + Sr1 - (M + I\Omega)]} \exp(r1Y) \\
 & - \frac{Gr(\exp(r1) - m)}{(\exp(r1) - \exp(r2))[r2^2 + Sr2 - (M + I\Omega)]} \exp(r2Y) \\
 & + \frac{1}{1 - \exp(r4 - r3)} \left[\frac{\alpha(\exp(r4 - r3) - \exp(-r3))}{M + I\Omega} \exp(I\Omega\tau) \right. \\
 & \quad \left. - \frac{Gr(m - \exp(r2))(\exp(r4 - r3) - \exp(r1 - r3))}{(\exp(r1) - \exp(r2))[r1^2 + Sr1 - (M + I\Omega)]} \right. \\
 & \quad \left. - \frac{Gr(\exp(r1) - m)(\exp(r4 - r3) - \exp(r2 - r3))}{(\exp(r1) - \exp(r2))[r2^2 + Sr2 - (M + I\Omega)]} \right] \exp(r3Y) \\
 & + \frac{1}{\exp(r4 - r3) - 1} \left[\frac{\alpha(1 - \exp(-r3))}{M + I\Omega} \exp(I\Omega\tau) \right. \\
 & \quad \left. - \frac{Gr(m - \exp(r2))(1 - \exp(r1 - r3))}{(\exp(r1) - \exp(r2))[r1^2 + Sr1 - (M + I\Omega)]} \right. \\
 & \quad \left. - \frac{Gr(\exp(r1) - m)(1 - \exp(r2 - r3))}{(\exp(r1) - \exp(r2))[r2^2 + Sr2 - (M + I\Omega)]} \right] \exp(r4Y),
 \end{aligned} \tag{3.4}$$

$$\theta = \frac{(m - \exp(r2))}{(\exp(r1) - \exp(r2))} \exp(r1Y) + \frac{(\exp(r1) - m)}{(\exp(r1) - \exp(r2))} \exp(r2Y), \tag{3.5}$$

where

$$\begin{aligned}
 r1, 2 &= -\frac{PrS}{2} \pm \sqrt{\frac{Pr^2S^2}{4} - Pr(H - I\Omega)}, \\
 r3, 4 &= -\frac{S}{2} \pm \sqrt{\frac{S^2}{4} + (M + I\Omega)}.
 \end{aligned}$$

The physical insights of the solutions (3.4, 3.5) are discussed in the next section. However, it is important to state here that from the physical point of view, it is necessary to know the skin friction or shear on the channel walls. By virtue of the non-dimensional quantities (2.8), it is given by

$$\tau_s = \frac{dU}{dY} \Big|_{Y=0,1}. \tag{3.6}$$

Knowing the temperature distribution, we can equally calculate the rate of heat flux, q_w , on the channel walls. This is calculated from

$$q_w = \frac{d\theta}{dY} \Big|_{Y=0,1}. \tag{3.7}$$

by virtue of equation (2.8). We note here that for brevity, the discussions of skin friction and the rate of heat flux are not presented.

4 Discussion of Results

The problem of MHD pulsatile flow through a channel with perforated or porous walls with heat generation has been examined. Analytical solutions (3.4, 3.5) are advanced to the governing

equations (2.9, 2.10) with the aid of the boundary conditions (2.11, 2.12). The discussions of the results are made via illustrative graphical representations based on certain range of values of the physical parameters entering the problem. The typical parameters entering the problem are m , wall temperature ratio; S , Suction parameter: $S > 0$, Suction and $S < 0$, Injection; M , Magnetic parameter; Gr , Grashof number: $Gr > 0$, cooling and $Gr < 0$ heating; H , Heat Source: $H > 0$, Heat generation and $H < 0$, Heat loss; Pr , Prandtl number.

The values of the Prandtl number, Pr chosen for the investigations are $Pr = 0.71$ for air, $Pr = 7.00$ for water and $Pr = 21.00$ for human blood. The physical significance of Prandtl number is that it is a measure of momentum and thermal buoyancy forces. It signifies the ratio of the momentum boundary layer thickness to the thermal boundary layer thickness. If $Pr = 1$, it signifies that the velocity and thermal boundary layers grow together, if $Pr > 1$, it signifies that the velocity boundary layer grows faster than the thermal boundary layer, and if $Pr < 1$, it signifies the opposite such that the thermal boundary layer grows faster than the momentum boundary layer. It is also known that a low Prandtl number (liquid metals) signifies that viscous effects are small, and a high Prandtl number (heavy oils) signifies that inertia effects are small (creeping flows).

In order to gain insights and understanding of the various physical parameters entering the problem for the interpretation of the figures presented in this paper, they must be viewed horizontally and vertically in the order in which they are appearing in the various figures, especially the parameters π and Ω and their effects to the flow variables U and θ vis-a-vis the other parameters Pr , Gr , H , M and S .

Fig. 1 depicts various velocity profiles for air, $Pr = 0.71$; water, $Pr = 7.00$ and human blood, $Pr = 21.00$ with values of the wall temperature ratio, $m = -1, 0, 1, 2$, keeping other parameters constant. It is clearly seen that as the Prandtl number increases the maximum height of the flow in the channel decreases. For $Pr = 0.71$ and $Pr = 7.00$ in particular for $\Omega = \pi/5$ and $\Omega = \pi/3$, the maximum velocity in the channel increases with increasing wall temperature ratio, m , and the occurrence of the maximum velocity is centred around the middle of the channel. While for $Pr = 21$ the maximum velocity is seen to be increasing with respect to increase in the wall temperature ratio in the case of $\Omega = \pi/5$. For π , the flow is seen negative in all $Pr = 0.71, Pr = 7$ and $Pr = 21$ with reversal effects displayed in $Pr = 7$ and $Pr = 21$ as m increases. Physically, the manifestations meet the general notion that fluids with large Prandtl number have high viscosity and small thermal conductivity, which makes the fluid thick, and hence causes a decrease in the velocity of the fluid. However, the wall temperature ratio plays an enhancing role, thereby increasing the velocity, completely opposite to the effect of the Prandtl number.

Figs. 2 and 3 display respectively profiles for the effect of Grashof number for $m = -1, 0$ and $m = 1, 2$. It is known that the Grashof number in natural convection controls the fluid flow. The Grashof number is a free convection parameter that signifies the ratio between a thermal buoyancy force due to spatial variation in the fluid density to the restraining hydrodynamic force due to the viscosity of the fluid. The values of the Grashof number in this investigation are all taken to be positive to represent the cooling of the lower plate temperature T_0 . Buoyancy force acts like a favourable pressure gradient that accelerates the fluid flow within the channel. As expected, it is seen that there is an increase in the velocity due to the increasing of the thermal buoyancy force, and the maximum velocity is seen to occur around the middle of the channel, which drifts toward the upper plate, especially for $m = 1, 2$ with $\Omega = \pi/5, \pi/3$. It must be emphasized here that when there are no free convection currents, $Gr = 0$, the flow in the channel is seen to be symmetric, but the maximum velocity decreases as Ω increases.

Figs. 4 and 5 represent the effect of heat source respectively for $m = -1, 0$ and $m = 1, 2$ with the heat source values $H = 0, 2, 4, 8$. It can be observed that with heat source in the model, the flow pattern within the channel is changed rather than being smooth, especially for those profiles resulting from $m = -1, 1, 2$ for $\Omega = \pi/5, \pi/3$.

Figs. 6 and 7 display the flow profiles with the human blood with various values of magnetic parameter. It is observed that for $m = -1, 0, 1, 2$ with $\Omega = \pi/5, \pi/3$, respectively, the maximum velocity decreases with increasing magnetic parameter. However, for $m = 1, 2$ with $\Omega = \pi/5, \pi/3$ displays a reversal of the effect of the magnetic parameter that exhibits negative maximum velocity at the centre of the channel as the magnetic parameter increases. The application of the transverse magnetic field plays the role of a resistive type of force simply known as Lorentz force similar to drag force that acts in the opposite direction of the fluid motion, which tends to resist the flow thereby reducing its velocity.

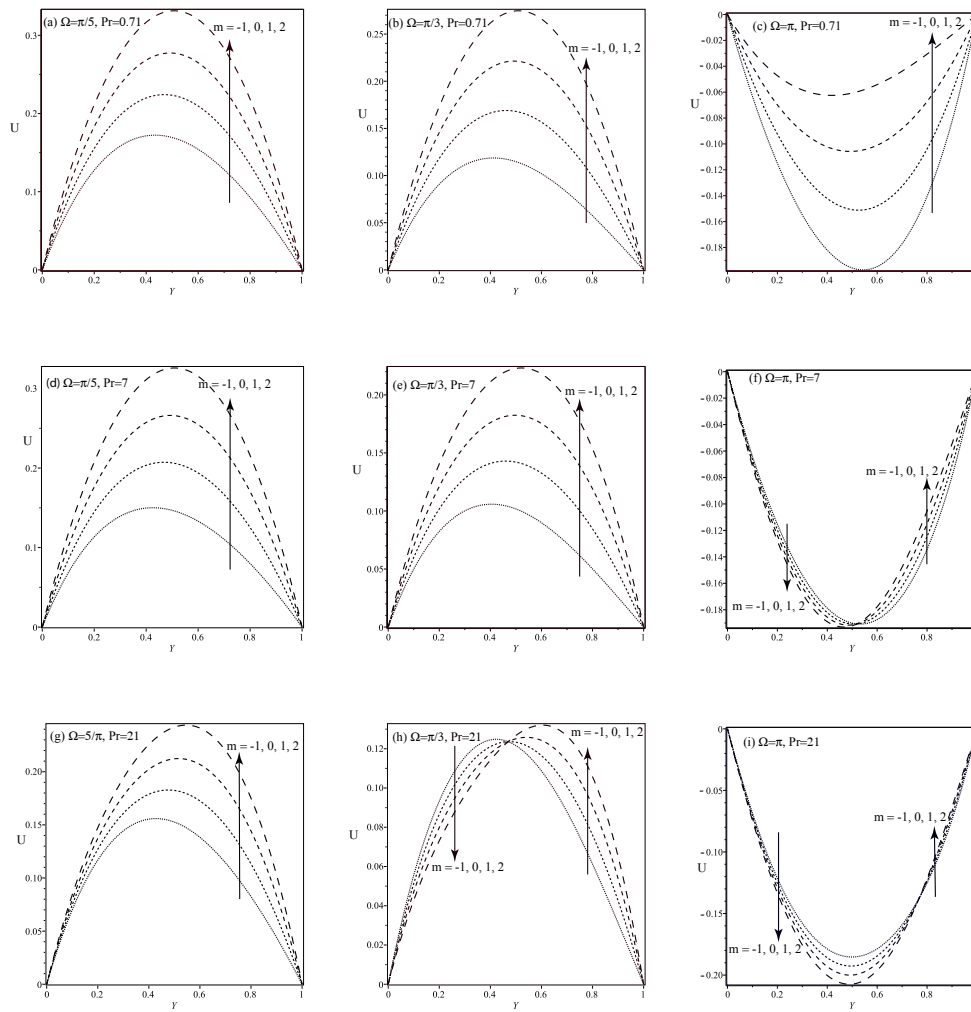


Fig. 1. Effects of Wall Temperature Ratio on Velocity Profiles for $Pr = 0.71$: (a) $\Omega = \pi/5$, (b) $\Omega = \pi/3$, (c) $\Omega = \pi$; $Pr = 7$: (d) $\Omega = \pi/5$, (e) $\Omega = \pi/3$, (f) $\Omega = \pi$; $Pr = 21$: (g) $\Omega = \pi/5$, (h) $\Omega = \pi/3$, (i) $\Omega = \pi$ with $S = 0.2, M = 2, Gr = 1, \tau = 1, H = 0.2, \alpha = 2$

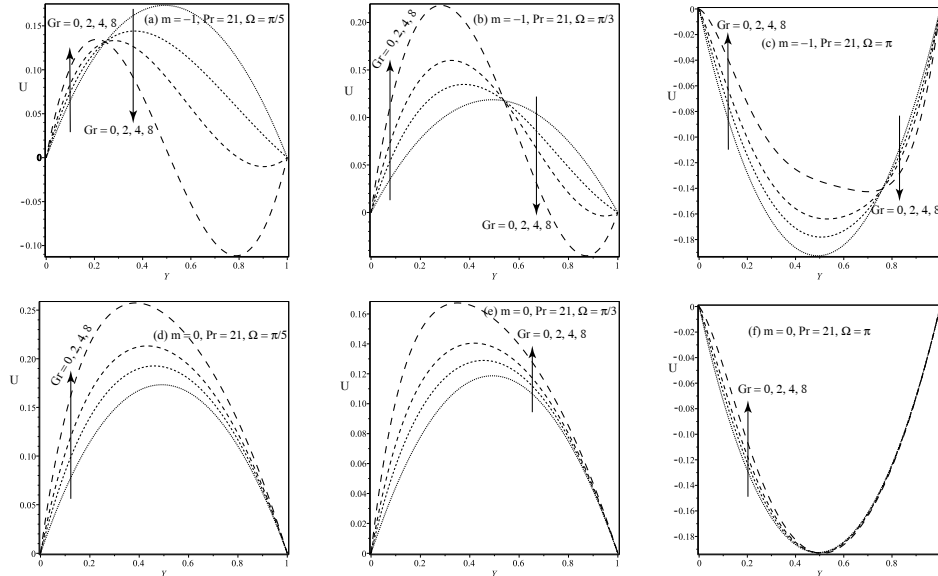


Fig. 2. Grashof Number on Velocity Profiles for $m = -1$, $Pr = 21$: (a) $\Omega = \pi/5$, (b) $\Omega = \pi/3$, (c) $\Omega = \pi$; $m = 0$, $Pr = 21$: (d) $\Omega = \pi/5$, (e) $\Omega = \pi/3$, (f) $\Omega = \pi$ with $S = 0.2, M = 2, \tau = 1, H = 0.2, \alpha = 2$

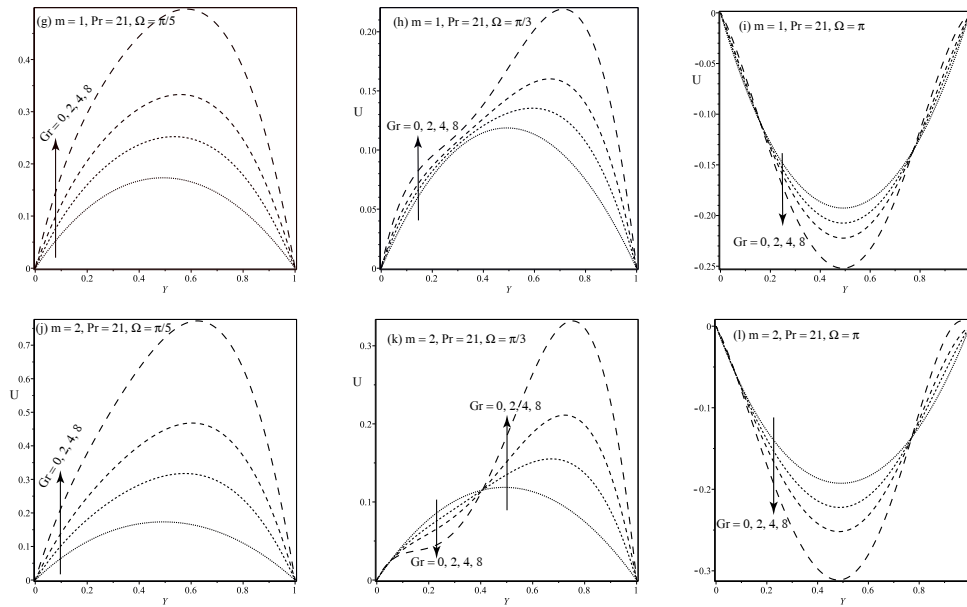


Fig. 3. Grashof Number on Velocity Profiles for $m = 1$, $Pr = 21$: (g) $\Omega = \pi/5$, (h) $\Omega = \pi/3$, (i) $\Omega = \pi$; $m = 2$, $Pr = 21$: (j) $\Omega = \pi/5$, (k) $\Omega = \pi/3$, (l) $\Omega = \pi$ with $S = 0.2, M = 2, \tau = 1, H = 0.2, \alpha = 2$.

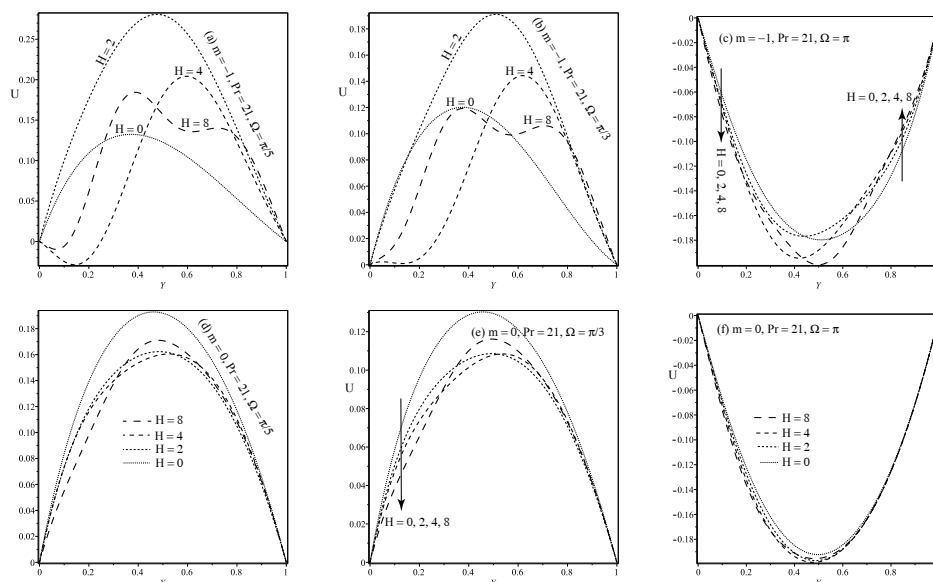


Fig. 4. Effect of Heat Source Parameter on Velocity Profiles for $m = -1, Pr = 21$: (a) $\Omega = \pi/5$, (b) $\Omega = \pi/3$, (c) $\Omega = \pi$; $m = 0, Pr = 21$: (d) $\Omega = \pi/5$, (e) $\Omega = \pi/3$, (f) $\Omega = \pi$ with $S = 0.2, M = 2, Gr = 1, \tau = 1, \alpha = 2$

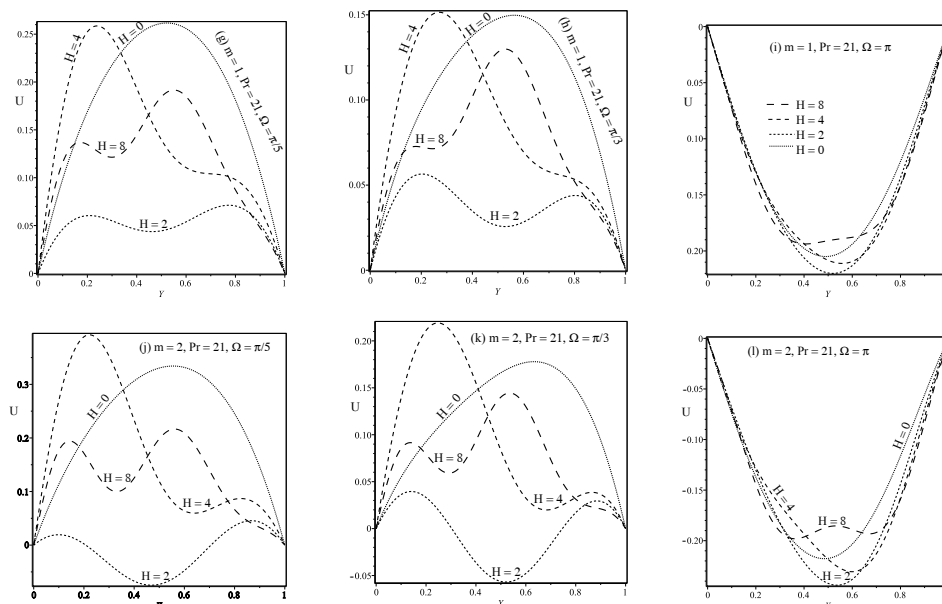


Fig. 5. Effect of Heat Source Parameter on Velocity Profiles for $m = 1, Pr = 21$: (g) $\Omega = \pi/5$, (h) $\Omega = \pi/3$, (i) $\Omega = \pi$; $m = 2, Pr = 21$: (j) $\Omega = \pi/5$, (k) $\Omega = \pi/3$, (l) $\Omega = \pi$ with $S = 0.2, M = 2, Gr = 1, \tau = 1, \alpha = 2$

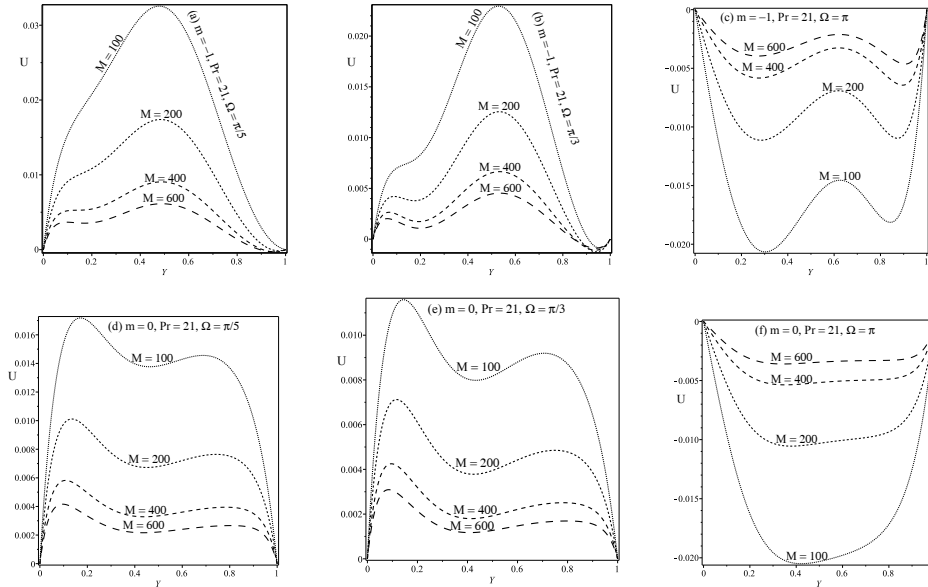


Fig. 6. Effect of Magnetic Parameter on Velocity Profiles for $m = -1, Pr = 21$: (a) $\Omega = \pi/5$, (b) $\Omega = \pi/3$, (c) $\Omega = \pi$; (II) $m = 0, Pr = 21$: (d) $\Omega = \pi/5$, (e) $\Omega = \pi/3$, (f) $\Omega = \pi$ with $S = 0.2, Gr = 1, \tau = 1, H = 0.2, \alpha = 2$

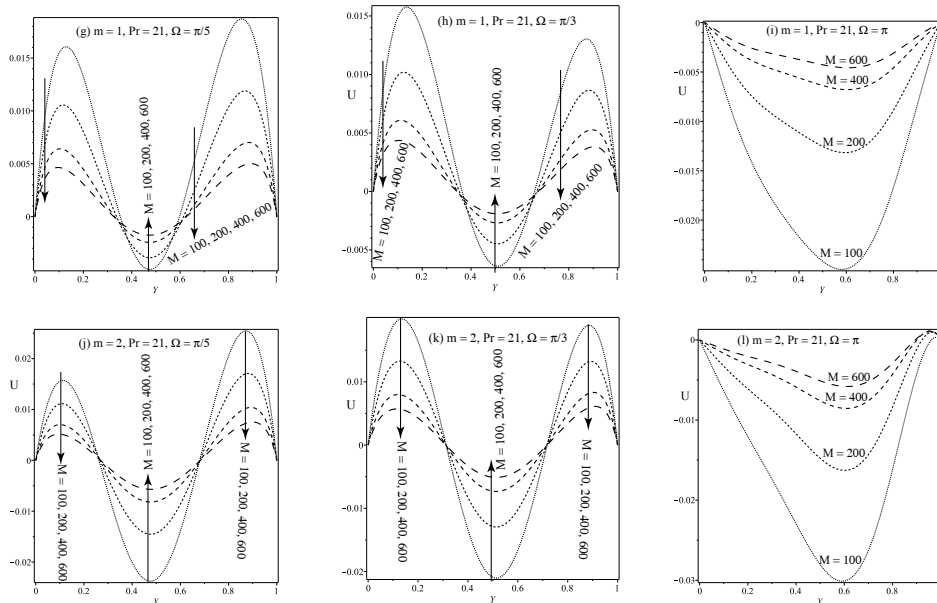


Fig. 7. Effect of Magnetic Parameter on Velocity Profiles for $m = 1, Pr = 21$: (g) $\Omega = \pi/5$, (h) $\Omega = \pi/3$, (i) $\Omega = \pi$; $m = 2, Pr = 21$: (j) $\Omega = \pi/5$, (k) $\Omega = \pi/3$, (l) $\Omega = \pi$ with $S = 0.2, Gr = 1, \tau = 1, H = 0.2, \alpha = 2$

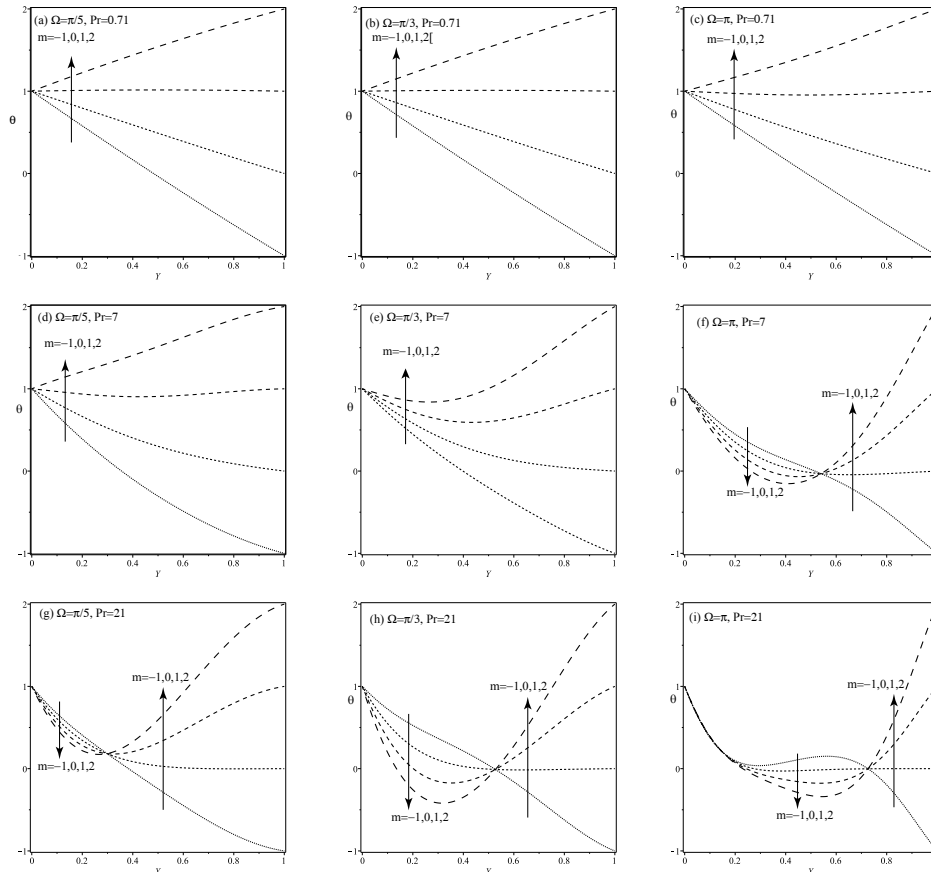


Fig. 8. Effects of Wall Temperature Ratio on Temperature Profiles for $Pr = 0.71$: (a) $\Omega = \pi/5$, (b) $\Omega = \pi/3$, (c) $\Omega = \pi$; $Pr = 7$: (d) $\Omega = \pi/5$, (e) $\Omega = \pi/3$, (f) $\Omega = \pi$; $Pr = 21$: (g) $\Omega = \pi/5$, (h) $\Omega = \pi/3$, (i) $\Omega = \pi$ with $S = 0.2, M = 2, Gr = 1, \tau = 1, H = 0.2, \alpha = 2$

Figs (8-10) delineate the effects of Wall temperature ratio m and Heat generation H parameters on the temperature with $Pr = 0.71, 7, 21$ and $\Omega = \pi/5, \pi/3, \pi$. The Prandtl number Pr , which associates the ratio of kinematic viscosity to thermal diffusivity, distorts the temperature towards the middle of the channel as it increases. This is well pronounced in the Fig. (8), especially for the cases of $Pr = 7$ and $Pr = 21$ with the human blood playing out more actively than the water as Ω increases.

Figs. (9) and (10) are temperature profiles due to the effect of Heat generation for human blood with the Wall temperature ratio. It is observed that heat generation produces more oscillations of the temperature in the fluid. Physically, large heat generation implies a large surface heat flux which leads to the increase in the number of oscillations of the temperature of the fluid. In all, the value of the lower channel temperature is seen as 1, while the upper assumes the value of the given Wall temperature ratio, satisfying the boundary conditions. It is clearly depicted that all other temperatures asymptote to the one for $H = 0$ with the oscillations demonstrating over and under shoots of the values of the temperature at the lower and upper channels.

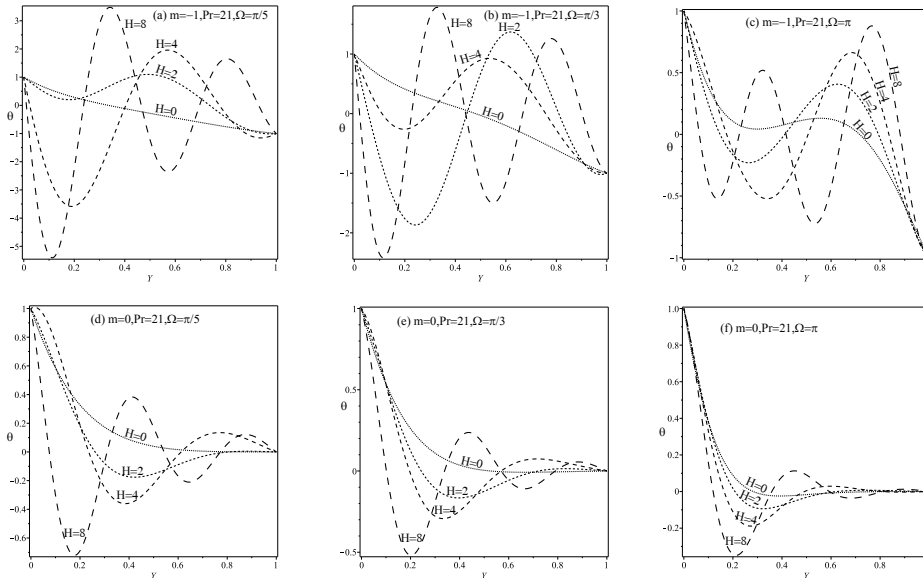


Fig. 9. Heat Generation Parameter on Temperature Profiles for $m = -1, Pr = 21$: (a) $\Omega = \pi/5$, (b) $\Omega = \pi/3$, (c) $\Omega = \pi$; (II) $m = 0, Pr = 21$: (d) $\Omega = \pi/5$, (e) $\Omega = \pi/3$, (f) $\Omega = \pi$ with $S = 0.2, M = 2, \tau = 1, H = 0.2, \alpha = 2$

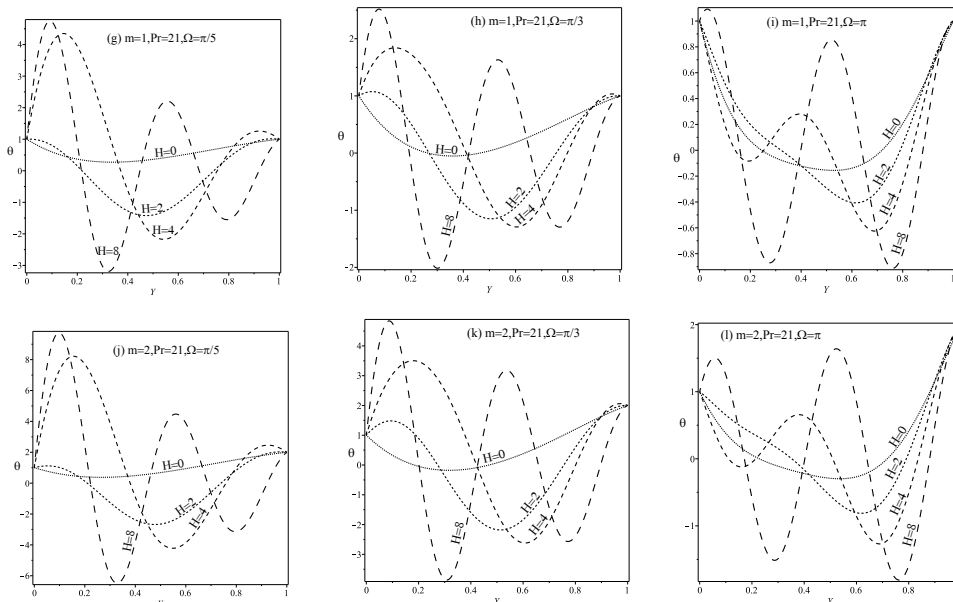


Fig. 10. Heat Generation Parameter on Temperature Profiles for $m = 1, Pr = 21$: (g) $\Omega = \pi/5$, (h) $\Omega = \pi/3$, (i) $\Omega = \pi$; $m = 2, Pr = 21$: (j) $\Omega = \pi/5$, (k) $\Omega = \pi/3$, (l) $\Omega = \pi$ with $S = 0.2, M = 2, \tau = 1, H = 0.2, \alpha = 2$

Table. 1. Values of Velocity determined at $Y = 0.5$ using $m = -1, 0, 1, 2$ for different values of both Suction, $S > 0$ and Injection, $S < 0$ for $Pr = 21, \alpha = 2 = Gr = M = H = 2, \tau = 1, \Omega = \pi/3$

m	$S = 0.2,$	$S = -0.2$	$S = 0.5,$	$S = -0.5$	$S = 0.8,$	$S = -0.8$	$S = 1.2,$	$S = -1.2$
-1	0.19098,	0.04626	0.85938,	-0.62309	-0.18111,	0.41568	-0.19556,	0.42668
0	0.10856,	0.03620	0.12174,	-0.61949	0.12040,	0.41880	0.11662,	0.49861
1	0.02614,	0.02614	-0.61590,	-0.61590	0.42191,	0.42191	0.49968,	0.49968
2	-0.05628,	0.01608	-1.35354,	-0.61231	0.72342,	0.42503	0.88273,	0.50074

Tables 1 and 2 depict respectively values of the velocity and temperature at the centre of the channel $Y = 0.5$ for different values of Suction, $S > 0$ and Injection, $S < 0$ with the respective values of the wall temperature ratio, $m = -1, 0, 1, 2$. From both tables, it is clearly observed that both Suction and Injection give an upturn or increase and a downturn or decrease to the velocity and temperature for $m = -1, 0$. Sectionally, the velocity and temperature experienced increase in the first two values of Suction, while in the last three, it experienced decrease. On the other hand, the opposite was the case for the effect of Injection on the velocity and temperature. For $m = 1, 2$, it is observed that Suction respectively Injection gives downturn to the velocity and temperature in the first two values, whereas upturn was seen in the last three. In all, it is evident that the range of the upturn effect of Suction and Injection on the velocity and temperature are much more than the downturn effect for both cases of $m = -1, 0$ and $m = 1, 2$. However, both effects are more pronounced in the temperature than the velocity. Physically, the upturn respectively the downturn signifies the oscillatory nature of the flow vis-a-vis the temperature initiated by the pressure gradient, just as the other parameters have already confirmed.

Table. 2. Values of Temperature determined at $Y = 0.5$ using $m = -1, 0, 1, 2$ for different values of Suction, $S > 0$ and Injection, $S < 0$ for $Pr = 21, \alpha = 2 = Gr = M = H, \tau = 1, \Omega = \pi/3$

m	$S = 0.2,$	$S = -0.2$	$S = 0.5,$	$S = -0.5$	$S = 0.8,$	$S = -0.8$	$S = 1.2,$	$S = -1.2$
-1	0.89806,	-0.89806	2.87553,	-2.87553	-2.21957,	2.21957	-1.85680,	1.85680
0	-0.12532,	-1.02338	-0.01517,	-2.89070	0.00050,	2.22007	0.00001,	2.09452
1	-1.14870,	-1.14870	-2.90587,	-2.90587	2.22057,	2.22057	2.09452,	2.09452
2	-2.17207,	-1.27401	-5.79657,	-2.92104	4.44064,	2.22107	4.18904,	2.09453

5 Concluding Remarks

The problem of MHD pulsatile flow through a channel with perforated walls and with heat generation has been examined. Analytical solutions of the flow variables are obtained via quasi-steady-state solution assumption initiated by the oscillatory pressure gradient term. Some physical parameters were identified entering the problem, which are used to discuss the results quantitatively with graphical illustrations. It is generally observed that the flow variables are significantly influenced by these parameters.

Among others, the primary findings are summarized as follows:

- 1) The maximum height of the flow and temperature in the fluid of the channel decreases with increasing Prandtl number, Pr ;
- 2) The maximum velocity in the channel increases with increasing wall temperature ratio, m ;
- 3) Reversal effects are seen displaced in the flow for $Pr > 0.71$;

- 4) That increasing thermal buoyancy force, Gr increases the velocity in the channel with reversal as the phase angle, Ω equals π ;
- 5) Increasing Magnetic parameter, M decreases maximum velocity in the channel with flow reversals seen near the centre of the channel;
- 6) Increasing Heat source, H introduces non-smooth flow in the maximum velocity with temperature oscillations in the fluid of the channel;
- 7) Both Suction, $S > 0$ and Injection, $S < 0$ introduced upturn and downturn of both the velocity and temperature, thereby physically signifying the oscillatory effect of the pressure gradient.

It is hoped that the results may serve as tool kit for comparisons to other analytical or semi-analytical methods such as Laplace Transform, Caputo-Fabrizio Fractional, and Adomian Decomposition Techniques vis-a-vis the verification of the efficiency and accuracy of numerical experimentations, particularly concerning researches geared towards the modelling of heat generation applications in industrial pollutions, bio-systems and hyperthermia studies.

Acknowledgement

The authors gratefully acknowledge the reviewers' comments that improved the quality of the article.

Competing Interests

Authors have declared that no competing interests exist.

References

- [1] Berman AS. Laminar flow in an annulus with porous walls. J Appl Phys; 1958;29:71-75.
- [2] Wang YC. Pulsatile flow in a Porous Channel. J Appl Mech; 1971;38:553-555.
- [3] Esmond WG, Clark H. Mathematical analysis and mass transfer optimization of a compact, low cost, pump system for hemodialysis (Dialung). Proc, Biomedical Fluid Mechanics Symp. AMSE, New York; 1966.
- [4] Misra JC, Shit GC, Rath HJ. Flow and heat transfer of a MHD viscoelastic Fluid in a Channel with Stretching Walls: Some Applications to Haemodynamics. Physics: Flu-dyn; 2010.
- [5] Vardanyan VA. Effect of magnetic field on blood flow. Biofizika. 1973;18(3):491-496.
- [6] Ali N, Khan SU, Abbas Z. Hydromagnetic flow and heat transfer of a jeffrey fluid over an oscillatory stretching surface. Zeitschrift fr Naturforschung A; 2015;70(7):567-576.
DOI: <https://doi.org/10.1515/zna-2014-0273>
- [7] Khan SU, Ali N, Abbas Z. Hydromagnetic Flow and Heat Transfer over a Porous Oscillating Stretching Surface in a Viscoelastic Fluid with Porous Medium. PLOS ONE. 2015;10(12):e0144299.
DOI: [10.1371/journal.pone.0144299](https://doi.org/10.1371/journal.pone.0144299)
- [8] Ali N, Khan SU, Abbas Z. Unsteady flow of third grade fluid over an oscillatory stretching sheet with thermal radiation and heat source/sink. Nonlinear Engineering. 2015;4(4):223-236.
DOI: <https://doi.org/10.1515/nleng-2015-0019>

- [9] Khan SU, Ali N, Abbas Z. Soret and dufour effects on hydromagnetic flow of viscoelastic fluid over porous oscillatory stretching sheet with thermal radiation. *Journal of the Brazilian Society of Mechanical Sciences and Engineering*. 2016;38:2533-2546.
- [10] Khan SU, Ali N, Abbas Z. Influence of heat generation/absorption with convective heat and mass conditions in unsteady flow of eyring powell nanofluid over porous oscillatory stretching surface. *Journal of Nanofluids*. 2016;5(3):351-362.
DOI: 10.1166/jon.2016.1224
- [11] Ali N, Khan SU, Sajid M, Abbas Z. MHD flow and heat transfer of couple stress fluid over an oscillatory stretching sheet with heat source/sink in porous medium. *Alexandria Engineering Journal*, 2016;55:915-924.
Available: <http://dx.doi.org/10.1016/j.aej.2016.02.018>
- [12] Khan SU, Ali N, Abbas Z. Soret and dufour effects on hydromagnetic flow of eyring-powell fluid over oscillatory stretching surface with heat generation/absorption and chemical reaction. *Thermal Science*; 2017.
DOI: 10.2298/TSCI150831018U
- [13] Ali N, Khan SU, Abbas Z. Slip effects in the hydromagnetic flow of a viscoelastic fluid through porous medium over a porous oscillatory stretching sheet. *Journal of Porous media*, 2017;20(3):1-14.
- [14] Khan SU, Ali N. Unsteady hydromagnetic flow of oldroyd-b fluid over an oscillatory stretching surface: A mathematical model. *Technical Sciences*. 2017;20(1):2017 (In Press).
- [15] Ali N, Ullah M, Sajid M, Khan SU. Application of Legendre wavelets method to parallel plate flow of a third grade fluid and forced convection in a porous duct. *Eur. Phys. J. Plus*. 2017;132:133.
DOI: 10.1140/epjp/i2017-11423-y
- [16] Dewhirst MW, Samulski TV. *Hyperthermia in the treatment for cancer*. Upjhon: Kalamazoo, MI; 1988.
- [17] Craciunescu OI, Clegg ST. Pulsatile blood flow effects on temperature distribution and heat transfer in rigid vessels. *J Biomech Engg*. 2001;123:500-5.
- [18] Weinbaun S, Jiji LM, Lemons DE. Theory and experiment for the effect of vascular microstructure on surface tissue heat transfer - Part I: Anatomical foundation and model conceptualization. *J Biomech Engg*. 1984;106:321-30.
- [19] Jiji LM, Weinbaun S, Lemons DE. Theory and experiment for the effect of vascular microstructure on surface tissue heat transfer - Part II: Model formulation and solution. *J Biomech Engg*. 1984;106:331-41.
- [20] Haq RU, Shahzad F, Al-Mdallal QM. MHD pulsatile flow of engine oil based carbon nanotubes between two concentric cylinders. *Results in Physics*. 2017;7:57-68.
- [21] Mebine P. Radiation effects on MHD couette flow with Heat transfer between two parallel plates, *global jour. Pure & Applied Mathematics*, 2007;3(2):191-202.

- [22] Burton AC. Physiology and biophysics of the circulation, introductory text. Year Book Medical Publishers, Chicago, Ill,USA; 1966.
- [23] Bestman AR. Pulsatile flow in heated porous channel. Int J Heat Mass Transfer. 1982;25(5):675-682.
- [24] Rubin H, Atkinson J. Environmental fluid mechanics. Marcel Dekker, Inc, New York; 2001.

© 2017 Mebine and Ebiwareme; This is an Open Access article distributed under the terms of the Creative Commons Attribution License (<http://creativecommons.org/licenses/by/4.0>), which permits unrestricted use, distribution, and reproduction in any medium, provided the original work is properly cited.

Peer-review history:

The peer review history for this paper can be accessed here (Please copy paste the total link in your browser address bar)

<http://sciencedomain.org/review-history/18651>